

2021-06

Foulweather friends: Modelling thermal stress mitigation by symbiotic endolithic microbes in a changing environment

Zardi, GI

<http://hdl.handle.net/10026.1/17480>

10.1111/gcb.15616

Global Change Biology

Wiley

All content in PEARL is protected by copyright law. Author manuscripts are made available in accordance with publisher policies. Please cite only the published version using the details provided on the item record or document. In the absence of an open licence (e.g. Creative Commons), permissions for further reuse of content should be sought from the publisher or author.

1 **Foul-weather friends: Modelling thermal stress mitigation by**
2 **symbiotic endolithic microbes in a changing environment**

3

4 Gerardo I. Zardi^{1#}, Jonathan R. Monsinjon^{1#}, Christopher D. McQuaid¹, Laurent Seuront^{1,2,3},
5 Mauricio Orostica¹, Andrew Want⁴, Louise B. Firth⁵, Katy R. Nicastro^{1,6*}

6

7 ¹Department of Zoology and Entomology, Rhodes University, Grahamstown 6140, South Africa

8 ²Univ. Lille, CNRS, Univ. Littoral Côte d'Opale, UMR 8187 – LOG – Laboratoire d'Océanologie et de
9 Géosciences, F-59000 Lille, France

10 ³Department of Marine Energy and Resources, Tokyo University of Marine Science and Technology,
11 4-5-7 Konan, Minato-ku, Tokyo 108-8477, Japan

12 ⁴International Centre for Island Technology, Heriot Watt University Orkney Campus, Robert Rendall
13 Building, Franklin Road, Stromness, Orkney, KW16 3AW

14 ⁵School of Biological and Marine Sciences, University of Plymouth, Plymouth, UK

15 ⁶CCMAR, CIMAR Associated Laboratory, University of Algarve, Campus de Gambelas, 8005-139
16 Faro, Portugal

17 #Equal contribution

18 *Corresponding author: e-mail: katynicastro@gmail.com, phone: +351 927738340

19

20

21 **Running title:** Thermal mitigation by symbiotic endoliths

22 **ABSTRACT**

23 Temperature extremes are predicted to intensify with climate change. These extremes are
24 rapidly emerging as a powerful driver of species distributional changes with the capacity to
25 disrupt the functioning and provision of services of entire ecosystems, particularly when they
26 challenge ecosystem engineers. The subsequent search for a robust framework to forecast
27 the consequences of these changes mostly ignores within-species variation in thermal
28 sensitivity. Such variation can be intrinsic, but can also reflect species interactions. Intertidal
29 mussels are important ecosystem engineers that host symbiotic endoliths in their shells. These
30 endoliths unexpectedly act as conditionally beneficial parasites that enhance the host's
31 resistance to intense heat stress. To understand how this relationship may develop under
32 environmental change, we examined the conditions under which it becomes advantageous by
33 reducing body temperature. We deployed biomimetic sensors, built using the shells of mussels
34 that were or were not infested by endoliths, at 9 European locations spanning a temperature
35 gradient across 22° of latitude (Orkney, Scotland to the Algarve, Portugal). Daily wind speed
36 and solar radiation explained the maximum variation in the difference in body temperature
37 between infested and non-infested mussels; the largest difference occurred under low wind
38 speed and high solar radiation. We inferred body temperature differences between infested
39 and non-infested mussels during known heatwaves that induced mass mortality of the mussel
40 *Mytilus edulis* along the French coast of the English Channel in summer 2018 to quantify the
41 thermal advantage of endolith infestation during temperature extremes. Under these
42 conditions, endoliths provided thermal buffering of between 1.7°C and 4.8°C. Our results
43 strongly suggest that sustainability of intertidal mussel beds will increasingly depend on the
44 thermal buffering provided by endoliths. More generally, this work shows that biomimetic
45 models indicate that within-species thermal sensitivity to global warming can be modulated by
46 species interactions, using an intertidal host-symbiont relationship as an example.

47

48 **Keywords:** mutualism, climate change, thermal tolerance, biophysical model, mussels.

49

50 INTRODUCTION

51 Globally, extreme temperature events have risen in frequency, strength and duration
52 (e.g., Oliver et al., 2018) and are predicted to become more severe with intensifying climate
53 variability (Fischer et al., 2010; Rahmstorf et al., 2011). Recently, extended periods of
54 anomalously high temperatures such as heatwaves have driven significant ecological changes
55 (e.g., Hughes et al., 2017; Smale et al., 2019; Wernberg et al., 2013). Given the serious
56 consequences for biodiversity and ecosystem functioning, there is increasing interest in
57 understanding variability in within-species thermal tolerance; we have yet to understand why
58 some individuals survive when conspecifics succumb to abrupt temperature increases. The
59 appreciation of such within-species variability will aid the prediction of long-term responses by
60 species as a whole. Identifying the full capacity of species to survive heatwaves and extreme
61 heat stress events may offer crucial insights into the stability of their ecological, and socio-
62 economic functions.

63 Intertidal ecosystems are among the most productive of ecosystems, supplying vital
64 services such as food production, stabilization of shorelines, capture of 'blue carbon', water
65 clearance, nutrient turnover and acting as nurseries for high-trophic level taxa (e.g., Costanza
66 et al., 1997; Macreadie et al., 2019; Raffaelli et al., 2012). Due to their daily exposure to both
67 aerial and marine conditions and their low thermal inertia compared to open-ocean waters,
68 these ecosystems are particularly vulnerable to extreme climatic events such as heatwaves
69 and coldwaves (Halpern et al., 2008). Heatwaves in particular, have drastic deleterious effects
70 on intertidal ecosystems globally. Heatwave-induced mass mortalities, local extinctions and
71 range contractions of numerous key benthic habitat-forming species (e.g., corals, seagrasses,
72 macroalgae, bivalves) have resulted in depleted local biodiversity, reduced carbon
73 sequestration and weakened natural coastal defences (Arias-Ortiz et al., 2018; Holbrook et
74 al., 2020). The damage caused by heatwaves also reduces the socioeconomic value of these

75 ecosystems by reducing recreational activities and tourism (e.g., Smale et al., 2019; Stillman,
76 2019) with major direct economic damage to recreational, artisanal and commercial fisheries
77 (e.g., FAO, 2020; Li et al., 2019).

78 Mussel die-offs induced by heatwaves exemplify the severe economic and ecological
79 effects of extreme heat events. Intertidal mussels are dominant ecosystem engineers that
80 provide crucial habitat, supporting biodiversity and underpinning myriad ecosystem functions
81 and services. For example, evidence from the NE Pacific coast and from southern African
82 rocky shores shows that hundreds of associated species (e.g. invertebrates, small fish and
83 algae) depend on mussel aggregations (Nicastro et al., 2020; Suchanek, 1985). Their dense
84 mono- and multi-layered beds remain moist and thermally benign during low tides and offer
85 protection against wave action during high tide (Helmuth et al., 2016). The loss of mussel beds
86 associated with recent warming trends has resulted in the decline of species richness and the
87 alteration of community structure (Harley, 2011).

88 Numerous experimental and observational studies have shown that symbiotic
89 interactions, both parasitic and mutualistic, have dramatic effects on the host organism
90 (Chomicki et al., 2020; Firth et al., 2017). Such interactions can alter the host's experience of
91 environmental stress by altering the host phenotype (Feldhaar, 2011), with consequences for
92 host fitness (i.e., survival and fecundity). When the host species is an ecosystem engineer,
93 such as a mussel, these interactions can have significant knock-on effects at population,
94 community and ecosystem levels (Fellous et al., 2009). As thermal stress intensifies under
95 climate change, the effect of symbionts on the temperature tolerance of their hosts will be
96 particularly important. Parasites can drive considerable alterations to both their host's thermal
97 performance optima (Gehman et al., 2018) and thermal preferences (Macnab et al., 2012). In
98 turn, mutualisms can favour survival following exposure to heat stress (Brumin et al., 2011;
99 Feldhaar, 2011). Because gradual warming and the increased stress of extreme heat events

100 will challenge individuals with and without symbionts, mutualistic relationships will have a
101 major role in setting within-species thermal variability (Feldhaar, 2011).

102 Critically, the nature of symbiotic associations is context dependent; a single symbiotic species
103 can have both positive and negative effects depending on the biotic/abiotic environment in
104 which the interaction occurs (e.g., Altizer et al., 2013; Harvell et al., 2009; Nowakowski et al.,
105 2016; Sauer et al., 2018). The gradual change between symbiotic states may confer a suite
106 of novel traits to the host organism thus offering it ecological opportunities (*sensu* Janson et
107 al., 2008) that would otherwise be unavailable. This is the case for the widespread symbiosis
108 between shell-degrading endolithic cyanobacteria and intertidal mussels (Zardi et al., 2016).
109 Until recently, numerous studies have described a multitude of negative (lethal and sub-lethal)
110 effects of endolith corrosion in mussels (Marquet et al., 2013), stressing the
111 parasitic nature of this relationship (Zardi et al., 2009). Endoliths are metabolically dependent
112 on the host for CO₂ released during shell degradation, which they use for photosynthesis
113 (Garcia-Pichel et al., 2010). As a result, endoliths can affect the host's energetic budgeting
114 through their boring activity at the expense of byssal attachment strength, growth and
115 reproduction (Kaehler et al., 1999; Marquet et al., 2013; Ndhlovu et al., 2021; Nicasro et al.,
116 2018; Zardi et al., 2009). Importantly, recent results have shown that shell corrosion caused
117 by endoliths mitigates the thermal stress experienced by their mussel hosts; mussels with
118 corroded shells experience significantly lower body temperatures leading to significant
119 increases in survival (up to 50%) during heatwaves compared to conspecifics that are not
120 affected by endoliths (Zardi et al., 2016). Such conditional help (*sensu* Fellous & Salvaudon,
121 2009) is triggered by reduced absorption of solar energy by mussel shells that are whitened
122 by endolithic boring (Gehman et al., 2019; Zardi et al., 2016).

123 Despite a growing number of studies reporting the incidence and effects of
124 phototrophic shell-degrading endoliths in a variety of taxa and habitats, the key environmental
125 factors that determine the nature of the relationship remain unknown. This study aims at
126 understanding the limits of endolith-mediated protection against thermal stress across

127 environments. Such knowledge is pivotal to the development of realistic, large-scale
128 predictions of how mussel beds will respond to environmental change and the consequences
129 to their related ecosystem and socio-economic value. To achieve this, we built biomimetic
130 temperature loggers using the shells of *Mytilus galloprovincialis* that were either heavily
131 infested or not infested by endoliths. These were then deployed in the field across a wide
132 latitudinal range (i.e., 37°N to 59°N) to assess changes in endolithic thermal buffering in a
133 variable environment and to identify the drivers of the maximum temperature differences
134 between non-infested and infested mussels. Data from the biomimetic temperature loggers
135 and high-resolution weather data were then used in Generalized Linear Mixed Models to
136 identify the environmental factors influencing the cooling effect of endoliths on mussel
137 populations. We subsequently used the model to identify maximum body temperature
138 differences between infested and non-infested mussels under the known conditions of a heat
139 wave-induced mortality event of *Mytilus edulis* that occurred along the north French coast in
140 summer 2018. In parallel, we assessed whether non-infested mussels warm up faster than
141 infested individuals as expected for dark ectotherms vs paler ones (Moyen et al., 2019; Porter
142 et al., 1969).

143

144 **METHODS**

145 **Drivers of the maximum temperature difference between non-infested and infested** 146 **mussels**

147 Biomimetic temperature loggers (robomussels) are used to mimic the thermal characteristics
148 of living mussels (Helmuth et al., 2010; Helmuth et al., 2016). In this study, robomussels were
149 deployed at multiple locations across a wide latitudinal range and environmental gradient
150 along North Atlantic shores to quantify differences in body temperatures of mussels with and
151 without endoliths when exposed to natural variability in meteorological conditions. All
152 robomussels were assembled using the emptied shells of *Mytilus galloprovincialis* (shell length

153 4-5 cm) sampled at Viana do Castelo (Portugal; 41°42'0.94"N, 8°51'25.59"W) from wave
154 exposed intertidal rocky shores composed of granite. Mussels were sampled within a
155 monolayered bed (i.e. all individuals attached directly to the substratum) in a sun-exposed
156 area (i.e. surfaces with limited shading, exposed to solar radiation 60 % of the day). Shells
157 were either non-infested (Group A; Zardi et al., 2009) or heavily infested by endoliths (Group
158 D; Fig. 1a); Group A shells have clean, intact periostracum and distinct periostracal striation,
159 Group D shells are severely pitted and deformed, and the outer striations on the periostracum
160 are almost completely absent. Robomussels were made by placing a temperature logger
161 (iButtons®, DS1922, Maxim Integrated Products, Dallas Semiconductor, USA, resolution =
162 0.5 °C, accuracy = 0.5 °C) between two empty mussel valves filled with silicone sealant and
163 leaving it to dry at air temperature for 48 hours before being deployed in trials (Nicastro et al.,
164 2012). Endoliths in infested shells were killed by keeping the mussel shells in boiling water for
165 an hour before assembling them (Zardi et al., 2016). Loggers recorded temperatures at 30-
166 min intervals from 1st August to 13th September 2017, for a period of 42 days at nine sites (Fig.
167 1b; Supplementary Table S1). Data were lost from Plymouth (UK) due to robomussels being
168 vandalised. For one site (Aberffraw, UK), deployment was done the following summer, from
169 28th July to 18th September 2018. At each site, three to six pairs of infested and non-infested
170 robomussels were glued to the substratum (Z-spar Splash zone, A-788) in the mid mussel
171 zone on a relatively flat slope, orientated like a living solitary mussel (i.e., longitudinal axis
172 oriented parallel to the substratum with the ventral side facing the substratum) and equidistant
173 from each other (approximately 10 cm).

174 At each site, average estimates of robomussel intertidal height were calculated using the
175 temperature logger profiles and tables of tidal heights (Gilman et al., 2006; Harley et al., 2003).
176 These profiles clearly reveal when robomussels are first inundated by the returning tide
177 through a sudden sharp drop in temperature. The time of tidal inundation was used to calculate
178 the Effective Shore Level (ESL) using the XTide software (<https://flaterco.com/xtide/>). Tidal
179 predictions were obtained for nearby maritime ports (Supplementary Table S2). For every

180 robomussel pair, we retrieved all tidal levels that were associated with a temperature drop of
181 $>8^{\circ}\text{C}$ in 30 min during incoming tides. We chose this threshold, which corresponds to a 5.33°C
182 drop in 20 min, to ensure reliability of ESL estimates while maximising the probability of finding
183 at least one drop during the study period (Gilman et al., 2006). We calculated the mean ESL
184 (\pm standard deviation; SD) for each robomussel pair (Supplementary Table S3). ESLs were
185 used to determine when mussels were exposed/submerged. However, ESLs can vary daily
186 due to surge and wave exposure, which might lead to the misidentification of
187 exposed/submerged periods. To ensure that temperature data were correctly attributed to
188 periods of submergence or aerial exposure, we kept data that were recorded above the upper
189 limit of a buffer zone (mean ESL + 0.3 m) or below the lower limit of a buffer zone (mean ESL
190 - 0.3 m). Temperature data during submergence were used as a control, as we expect no
191 differences in temperature between non-infested and infested robomussels when submerged.
192 We used Linear Mixed Effects models (LMEs; using 'nlme' R package; Pinheiro et al., 2020)
193 to test this. After adding robomussel identity as a random effect and controlling for
194 autocorrelation (autoregressive model of order 1), we found that non-infested mussels were,
195 on average, significantly warmer than infested ones during aerial exposure (mean difference
196 = 0.36°C , SD = 2.04, $t = -2.14029$, $p = 0.0323$) whereas we did not find a significant difference
197 during submergence ($t = -1.62900$, $p = 0.1033$). Therefore, we kept only temperature data
198 during emergence for further analysis.

199 Using robomussels as proxy for mussel body temperature (Helmuth et al., 2010;
200 Helmuth et al., 2016), we expected the maximum difference between non-infested and
201 infested mussels (calculated as non-infested minus infested temperatures for each
202 robomussel pair) to vary geographically during emergence due to site-specific meteorological
203 conditions. Meteorological variables that are considered determinants of the body temperature
204 of invertebrates (i.e. air temperature, wind speed, precipitation, relative humidity, and solar
205 radiation (Helmuth, 1998)) were obtained from nearby weather stations (Supplementary Table

206 S4). However, we excluded three of our nine study sites from this analysis because solar
207 radiation was not measured at these sites during the study period (Supplementary Table S4).
208 Weather station data in the United Kingdom (Met Office, 2019a, 2019b, 2019c), France and
209 Portugal were provided by the Centre for Environmental Data Analysis (CEDA;
210 <http://data.ceda.ac.uk/badc/ukmo-midas-open/data/>), Météo-France
211 (<https://donneespubliques.meteofrance.fr/>) and Instituto Português do Mar e da Atmosfera
212 (IPMA; <https://www.ipma.pt/en/otempo/obs.superficie/>), respectively.

213 We used Generalized Linear Mixed Models (GLMMs; using 'lme4' R package; Bates et
214 al., 2015) to test for effects of daily values of (i) mean air temperature ($^{\circ}\text{C}$), (ii) mean wind
215 speed (m s^{-1}), (iii) total precipitation (mm), (iv) mean relative humidity (%), and (v) total (global)
216 solar radiation (J m^{-2}) on the daily maximum difference in temperature between non-infested
217 and infested robomussels during emergence. Meteorological variables were averaged (or
218 summed for solar radiation and precipitation) within robomussel pair-specific periods of
219 emergence. The identity of individual pairs of robomussels was included as a random factor
220 nested within study site to account for inter- and intra-site variance. Because our dependant
221 variable was non-normally distributed (positively skewed), we used GLMMs with a Gamma
222 distribution and excluded the few days during which non-positive temperature differences
223 were found between paired robomussels. We applied a log link function to stabilize the
224 variance of residuals. We fitted all models (i.e. all combinations of response variables) using
225 maximum likelihood and selected the best candidates based on the lowest value of Akaike
226 Information Criteria corrected for finite sample size (AICc) and Akaike weights, which give a
227 measure of the relative support for each model (Akaike, 1974; Burnham et al., 2002). We
228 considered models with $\Delta\text{AICc} < 2$ as competitive and, for the sake of parsimony, we retained
229 the model with the least number of parameters. Based on this model, we extrapolated daily
230 maximum differences in body temperature between non-infested and infested mussels under
231 a range of meteorological conditions likely to be encountered on the shore.

232 **Quantifying the thermal advantage of infestation during a heatwave-induced mussel**
233 **mortality event**

234 To assess the extent of thermal buffering provided by endoliths during extreme hot weather
235 conditions, we used the meteorological data at Wimereux, France, during summer 2018 where
236 mass mortality events of *Mytilus edulis* occurred following heatwaves (Seuront et al., 2019).
237 Nine heatwaves (ranging from moderate to severe; see Table 2) were identified based on air
238 temperature, following Hobday et al. (2018). We extracted meteorological data during these
239 periods and predicted the daily maximum temperature difference between non-infested and
240 infested mussels based on the previously selected model.

241 **Assessing heating rate and maximum body temperature during aerial exposure**

242 Temperatures recorded by robomussels were used as proxy of the body temperatures of living
243 mussels. To assess whether non-infested mussels warm up faster and reach higher body
244 temperatures than infested ones during aerial exposure, we calculated the rate of change in
245 body temperature as well as the maximum and near-maximum (95th percentile) body
246 temperature for each robomussel during aerial exposure for every tidal cycle. We calculated
247 the average rate of change in body temperature during one tidal cycle using the slope of the
248 linear regression between temperature and time data (converted to °C h⁻¹). A positive slope
249 indicates that robomussels were warming up while a negative one indicates that robomussels
250 were cooling down. We assessed potential differences between non-infested mussels and
251 infested ones using Linear Mixed Effects models with robomussel identity included as a
252 random effect.

253

254 **RESULTS**

255 **The thermal buffering effect of infestation depends on solar radiation and wind speed**

256 Five candidate models were retained, with the number of selected meteorological parameters
257 varying from two to four (Table 1). When compared to the null model (i.e., assuming no effect
258 of any meteorological parameters; Table 1), these models exhibit a better fit (Table 1). The
259 two best models (i.e., those with the lowest AICc values) showed similar relative support
260 (Akaike weights > 0.2; Table 1) and, for the sake of parsimony, we selected the simplest one
261 (i.e., using solar radiation and wind speed; Table 1) for further analysis. The results suggest
262 that solar radiation ($t = 8.609$, $p < 0.0001$) and wind speed ($t = -3.181$, $p = 0.00147$) are the
263 main drivers of the maximum difference in body temperature between non-infested and
264 infested mussels. The selected model appropriately reproduced measured temperature
265 differences, albeit slightly underestimating the difference at high temperatures
266 (Supplementary Fig. S1). On average, daily total solar radiation during emergence increased
267 from northern to southern sites with greater variability measured at the three northernmost
268 (NEB, SKA and ABE) and intermediate (WIM) sites considered (Fig. 1c). Daily mean wind
269 speed showed the opposite trend; decreasing to the south and again with greater variability
270 measured at the three northernmost sites. Note that the southernmost site (VIL) was more
271 exposed to wind than the other southern site (MON) during the study period. Geographically,
272 the cooling effect of microbial endoliths (expressed as the maximum difference in body
273 temperature between non-infested and infested robomussels predicted from the selected
274 model using solar radiation and wind speed averaged over the study period) showed a
275 gradient decreasing from southern (VIL and MON) to intermediate (WIM) and northern (NEB,
276 SKA and ABE) sites (Fig. 1d). However, there was no clear pattern with latitude among the
277 closest sites (e.g., MON and VIL). Confidence intervals of predictions (Fig. 1d) are shown in
278 Supplementary Fig. S2 and the relationship between measured temperature differences and
279 weather data is shown in Supplementary Fig. S3.

280

281 **Prediction of body temperature differences between non-infested and infested mussels**
282 **during heatwaves**

283 In summer 2018 at Wimereux, based on the model that uses solar radiation and wind speed
284 (see Table 1 and prediction surface in Fig. 1d), we predicted a cooling effect of microbial
285 endoliths (i.e., the temperature difference between non-infested and infested mussels) of 4.21
286 to 4.77°C during June heatwaves (which were classified as moderate to strong), of 2.75 to
287 4.14°C during July heatwaves (which were classified as moderate to severe), and of 1.67 to
288 3.97°C during August heatwaves (which were classified as moderate to strong; estimates are
289 plotted on the prediction surface in Fig. 1d and confidence intervals are provided in Table 2).
290 During most of these heatwaves, mussels were exposed to high solar radiation (noticeably
291 higher than the conditions observed on average in southern sites like MON and VIL) and
292 moderate wind speeds (similar to the conditions observed on average at all sites except ABE
293 and MON; Fig. 1d). For one heatwave (10th August) that occurred under moderate solar
294 radiation and high wind speed, the predicted temperature difference was rather low and similar
295 to the ones predicted for northern sites (NEB, SKA and ABE).

296

297 **Non-infested mussels warm up faster and reach higher body temperatures than** 298 **infested mussels**

299 During periods of aerial exposure, non-infested robomussels warmed up faster than infested
300 ones ($t = -1.982$, $p = 0.0475$; mean rate of change = 0.38 and 0.28 °C h⁻¹, SD = 1.75 and 1.45,
301 respectively; Fig. 2a). Non-infested robomussels also reached higher maximum temperatures
302 than infested ones ($t = -4.477$, $p < 0.0001$; mean maximum temperature = 22.93 and 22.07°C,
303 SD = 7.5 and 6.6, respectively; Fig. 2b). We obtained similar results when comparing near-
304 maximum (95th percentile) temperatures ($t = -4.098363$, $p < 0.0001$; mean near-maximum
305 temperature = 22.47 and 21.69°C, SD = 7.31 and 6.45, respectively for non-infested and
306 infested ones; Fig. 2c).

307

308 **DISCUSSION**

309 We observed striking reductions in temperature in endolithically corroded robomussels
310 compared to uncorroded ones in intertidal habitats, across large geographical areas exposed
311 to a wide range of oceanographic and climatic conditions. Given that the biomimics used in
312 this study have been extensively shown to be an accurate tool for recording organismal body
313 temperature in their natural environment (e.g., Fitzhenry et al., 2004; Helmuth et al., 2016;
314 Seabra et al., 2015), our results can effectively be interpreted as a marked cooling effect in
315 infested mussels compared to non-infested mussels. Intraspecific variability in body
316 temperature has to be accounted for in order to interpret and predict responses of the species
317 to climatic change across biogeographic ranges. This is relevant not only for the individuals
318 themselves, but also for the ecosystem as it provides crucial insights into the future stability of
319 mussel beds and their role as ecosystem engineers that support myriad species, and a range
320 of ecosystem functions and services.

321 We identify daily-mean wind speed and daily-total solar radiation as the environmental
322 variables with the strongest influence on the within-site thermal buffering effects of endoliths.
323 This is in agreement with previous work showing how body temperatures of intertidal
324 ectothermic animals are primarily controlled by non-climatic heat sources, solar heating and
325 re-radiation as opposed to climatic heat sources, i.e. air and water temperatures (e.g.,
326 Helmuth, 2002; Marshall et al., 2010). Our results show a negative relationship between the
327 two key variables, suggesting that the seasonality of wind and solar radiation most likely will
328 shape the implications of our results. While the highest wind speeds typically occur during
329 winter, the peak in solar radiation usually occurs in summer when thermal heat stress is at its
330 highest. This means that the maximum endolithic thermal buffering occurs in summer when it
331 is also most ecologically meaningful. In summer, during heatwave conditions recorded at
332 Wimereux in France, body temperature differences between non-infested and infested
333 mussels ranged between 1.7°C and 4.8°C. Like other intertidal organisms, mussels live close

334 to the upper limit of their physiological thermal tolerance window and such a remarkable level
335 of thermal buffering due to phenotypic variation has the potential to trigger changes at the
336 population level, particularly in areas where the survival and physiological performance of
337 mussels have already been affected by increasing temperatures. Our findings show that
338 uncorroded individuals have significantly higher maximum body temperature and faster
339 heating rates than those of corroded mussels. In particular, heating rate is known to have
340 significant effects on cardiac thermal performance in intertidal mussels; recent studies show
341 that faster heating rates significantly increase the heart's critical temperature (i.e., the
342 temperature triggering a precipitous decline of heart rate; Moyen et al., 2019). Critically, these
343 studies also emphasise the complexity of abiotic and physiological interactions. Heating rates
344 significantly affect the cardiac thermal tolerance, of high- but not low-zone mussels, while
345 heavy mussels tend to heat up faster compared to light weight mussels- but at the fast-heating
346 rate only.

347 The heating rates recorded in our study are lower than those previously reported in
348 natural populations (e.g., Miller et al., 2017) or in laboratory experiments (e.g., Moyen et al.,
349 2019 and references therein) and are thus unlikely to significantly affect heart rates, at least
350 under our study conditions. Additionally, all mussels used to build robomussels were collected
351 from the same site and mussel zone and had similar shell length, excluding any potential effect
352 of body mass. Nevertheless, given the determinant role of intertidal height on mussel cardiac
353 thermal tolerance, further investigation is needed to assess the effect of endolithic corrosion
354 on heating rates and heart rates throughout the intertidal distribution of mussels and for
355 different body masses. Framed in a more theoretical context, our results show that endoliths
356 provide their host mussels with a *key innovation* (i.e., thermal buffering) that potentially offers
357 an ecological opportunity, opening previously unexploited niches. Key innovations (termed "*ad*
358 *hoc novelty*" in Feldhaar, 2011; Miller, 1949) are features that allow a species to interact with
359 the environment in a different way and thus may provide the capacity, otherwise unavailable,

360 to exploit available resources (Galis, 2001; Hunter, 1998; Rabosky, 2014). For instance, in
361 tropical dendrobatid poison frogs, the evolution of bright coloration as an advertisement of
362 unprofitability to predators, reduces the function and thus the need for predator-induced
363 “hiding” behaviour, thus offering novel habitat opportunities (Arbuckle et al., 2015; Santos et
364 al., 2003; Summers, 2003). Another example is that of archer fish (*Toxotes* spp.) in which the
365 evolved capacity to fire jets of water from their mouths to dislodge insects perched on
366 overhanging foliage has opened access to new prey resources (Burnette et al., 2015;
367 Schuster et al., 2006). Key innovations have been mainly investigated in an evolutionary
368 context and are often described as a key and eventually an essential stimulus for adaptive
369 radiation through “*the evolutionary divergence of members of a single phylogenetic lineage*
370 *into a variety of different adaptive forms*” (Futuyma et al., 1988).

371 However, key innovations can be obtained through faster or even non-evolutionary
372 routes. For instance, a variety of genome-engineering approaches have been used to reduce
373 the proportion of black found on dairy cattle coats aiming at decreasing radiative heat gain, a
374 contributing feature to heat stress (Maga, 2020). Similarly, alteration of a host’s life history
375 traits triggered by symbionts may become advantageous under certain environmental
376 conditions; fast-tracking the host to higher fitness levels that would otherwise be accessible
377 only through slower microevolutionary steps (Fellous & Salvaudon, 2009). Alternatively,
378 symbiont-induced phenotypic changes may provide new functions allowing the host to reach
379 higher levels of fitness unlikely to be attainable through mutation. Shell colour in intertidal
380 mussel is reasonably plastic, however, the distinctive shell whitening caused by the eroding
381 activity of endoliths extends beyond the range of such plasticity. This pronounced phenotypic
382 change provides mussels with a higher degree of thermal buffering that is most likely
383 unreachable through adaptive mutation. It has been suggested that endolithic thermal
384 buffering might be indicative of a transition towards mutualism in the endolith-mussel
385 relationship (Gehman & Harley, 2019; Zardi et al., 2016). Indeed, most mutualisms have
386 evolved from wholly parasitic associations and conditionally beneficial parasites are

387 intermediate stages in a transient relationship triggered by changes in the biotic/abiotic
388 environment (Fellous & Salvaudon, 2009). The ecological advantages of endolithic infestation
389 are likely to be increasingly important in an era of global warming and more frequent and
390 intense heatwaves. On the other hand, recurred storm strikes are also predicted to increase
391 potentially raising mortality rates in infested mussels as they are more weakly attached to
392 rocky shores than non-infested mussels. Critically, the ecological advantages of mussels with
393 corroded shells will vary spatially and temporally. Our results suggest that these benefits will
394 potentially peak in summer and at lower latitudes when and where intense solar radiation
395 maximises relative differences in body temperature between corroded and uncorroded
396 mussels.

397 In order to standardise our experimental design, all robomussels used were built using
398 *M. galloprovincialis* shells sampled from a single location in southern Portugal. In reality, our
399 study sites supported different mussel species, including *M. galloprovincialis*/*M. edulis* hybrids
400 in the UK and northern France (Bierne et al., 2003), raising the possibility that endolithic
401 communities and the cooling effect observed in *M. galloprovincialis* robomussels may not
402 apply to other species. Recent evidence indicates that endolithic community composition and
403 the thermal benefits they confer are similar among hosts. *Perna perna*, with an aragonite shell
404 and *M. galloprovincialis*, with aragonite and calcite shell layers, co-exist in South Africa.
405 Despite differences in shell and periostracum structure (Bers et al., 2010), severely infested
406 mussels of the two species support the same endolith species (Ndhlovu et al., 2020). Most
407 importantly, both mussels exhibit the same degree of thermal buffering by endoliths under a
408 variety of environmental conditions (Zardi et al., 2016). Together these findings support the
409 abundant literature highlighting the generalist, nonspecific, nature of endolithic corrosion (e.g.,
410 Golubic et al., 2005) and strongly suggest that thermal stress mitigation by symbiotic endolithic
411 microbes does not apply to *M. galloprovincialis* only.

412 Mussel mass mortalities have repeatedly been reported globally and are often attributed to
413 heatwaves (Harley, 2008; Petes et al., 2007; Suchanek, 1985; Tsuchiya, 1983). During the heatwave on
414 the northern French coastline in August 2018, large numbers of empty mussel shells were washed
415 ashore (Seuront et al., 2019). Interestingly, a close examination to over 1200 randomly shells collected
416 following this mass mortality event show that the vast majority of them (96 to 100%) had no sign of
417 infestation (Seuront, unpublished data, see Supplementary Material Figure S4). Although such
418 observations cannot quantify or confirm the protective roles of endoliths, they complement previous
419 field manipulative experiments in different regions showing that, during heat waves, the moderation
420 of solar heating by endoliths results in significantly lower mortality rates (Gehman & Harley, 2019;
421 Zardi et al., 2016). Interestingly, large-scale sampling covering a wide latitudinal range (ca. 28-37°N)
422 along the coasts of Portugal and Morocco revealed a strong gradient of increasing endolithic
423 infestation of *M. galloprovincialis* towards lower latitudes, presumably due to the enhancement of
424 endolith photosynthetic activity through greater light availability and decreased cloud cover towards
425 the equator (Lourenço et al., 2017). Importantly, *M. galloprovincialis* is the only *Mytilus* spp. along this
426 coast, eliminating potential confounding effects between endolith frequency and host identity.
427 Likewise, higher levels of shell corrosion at lower latitudes is unlikely due to latitudinal or geographic
428 changes in endolithic species. Endolithic community composition does not differ significantly between
429 *M. galloprovincialis* from native (Portugal) and invasive (South Africa) regions nor from *P. perna* shells
430 from different bioregion along 1000s km of the South African coast (Marquet et al., 2013; Ndhlovu et
431 al., 2019). Most importantly, our results indicate that endolithic corrosion is higher at lower
432 latitudes where its beneficial effects are enhanced and most beneficial to the host. Will climate-
433 associated thermal stress push the endolith-mussel relationship towards a long-lasting
434 mutually beneficial association? This seems possible as heatwaves are increasing in intensity,
435 frequency and duration and these trends are expected to strengthen under future climatic
436 changes (Perkins-Kirkpatrick et al., 2020; Smale et al., 2019). Further work is required to

437 evaluate if the cooling effect of endoliths has a significant impact on mussel fitness and if the
438 average fitness of corroded hosts, across all possible environments, is higher than that of
439 uncorroded individuals. Such an approach will also be key to testing the validity of near-future
440 conditions under which mussels shift their ecological niche to one whereby endoliths are more
441 often advantageous or might even evolve endolith dependence, losing the ability to live without
442 their symbionts.

443

444 Although hosts and symbionts have coupled life cycles, they can respond differently to
445 environmental changes. Thus, the response of host–symbiont interactions to climate warming
446 may largely depend on the performance of each interactor and the influence of the symbiont
447 on host performance (Gehman et al., 2018; Lafferty et al., 2003). In this context, mussel
448 survival may increasingly benefit from the thermal buffering provided by endolithic shell
449 erosion, which is predicted to increase as a result of ongoing ocean acidification and warming
450 rates (Reyes-Nivia et al., 2013; Tribollet et al., 2009). A further complication lies in the fact that
451 the endoliths infesting mussel shells comprise a community, the composition of which alters
452 in time and space (Ndhlovu et al., 2019; Pittera et al., 2014). Nevertheless, the generalist
453 nature of endoliths and their ubiquitous erosion of marine calcifying organisms
454 already stretched to the limits of their thermal tolerances strongly suggest that they will have
455 a key influence on the ability of many intertidal ecosystems to maintain their ecological
456 functions.

457

458 **ACKNOWLEDGEMENTS**

459 This work has also been financially supported by a Pierre Hubert Curien PESSOA Fellowship,
460 projects UIDB/04326/2020 from the Fundação para a Ciência e Tecnologia (FCT-MEC,
461 Portugal) and Grant number 64801 from the National Research Foundation of South Africa,
462 and a South African Research Chairs Initiative (SARChI) of the Department of Science and

463 Technology and the National Foundation and a scholarship from the South African National
464 Research Foundation (NRF). This work is a contribution to the CPER research project
465 CLIMIBIO. The authors thank the French Ministère de l'Enseignement Supérieur et de la
466 Recherche, the Hauts de France Region and the European Funds for Regional Economical
467 Development for their financial support for this project.

468

469 REFERENCES

470 Akaike, H. (1974). A new look at the statistical model identification. *IEEE Transactions on*
471 *Automatic Control*, 19, 716-723.

472 Altizer, S., Ostfeld, R. S., Johnson, P. T., Kutz, S., & Harvell, C. D. (2013). Climate change
473 and infectious diseases: from evidence to a predictive framework. *Science*,
474 341(6145), 514-519.

475 Arbuckle, K., & Speed, M. P. (2015). Antipredator defenses predict diversification rates.
476 *Proceedings of the National Academy of Sciences*, 112(44), 13597-13602.

477 Arias-Ortiz, A., Serrano, O., Masqué, P., Lavery, P. S., Mueller, U., Kendrick, G. A., . . .
478 Duarte, C. M. (2018). A marine heatwave drives massive losses from the world's
479 largest seagrass carbon stocks. *Nature Climate Change*, 8(4), 338-344.
480 doi:10.1038/s41558-018-0096-y

481 Bates, D., Mächler, M., Bolker, B., & Walker, S. (2015). Fitting linear mixed-effects models
482 using lme4. *Journal of Statistical Software*, 67(1), 1-48. doi:10.18637/jss.v067.i01

483 Bers, A., Díaz, E., Da Gama, B., Vieira-Silva, F., Dobretsov 3, S., Valdivia 4, N., . . . Sudgen
484 6, H. (2010). Relevance of mytilid shell microtopographies for fouling defence—a
485 global comparison. *Biofouling*, 26(3), 367-377.

486 Bierne, N., Borsa, P., Daguin, C., Jollivet, D., Viard, F., Bonhomme, F., & David, P. (2003).
487 Introgression patterns in the mosaic hybrid zone between *Mytilus edulis* and *M.*
488 *galloprovincialis*. *Molecular Ecology*, 12(2), 447-461.

489 Brumin, M., Kontsedalov, S., & Ghanim, M. (2011). Rickettsia influences thermotolerance in
490 the whitefly Bemisia tabaci B biotype. *Insect Science*, 18(1), 57-66.

- 491 Burnette, M. F., & Ashley-Ross, M. A. (2015). One shot, one kill: the forces delivered by
492 archer fish shots to distant targets. *Zoology*, 118(5), 302-311.
- 493 Burnham, K. P., & Anderson, D. R. (2002). *Model selection and multimodel inference: A*
494 *practical information-theoretic approach*. New York: Springer-Verlag.
- 495 Chomicki, G., Kiers, E. T., & Renner, S. S. (2020). The evolution of mutualistic dependence.
496 *Annual Review of Ecology, Evolution, and Systematics*, 51.
- 497 Costanza, R., d'Arge, R., De Groot, R., Farber, S., Grasso, M., Hannon, B., . . . Paruelo, J.
498 (1997). The value of the world's ecosystem services and natural capital. *nature*,
499 387(6630), 253-260.
- 500 FAO. (2020). *GLOBEFISH Highlights - A quarterly update on world seafood markets. with*
501 *Jan. – Jun. 2019 Statistics – A quarterly update on world seafood markets*. Retrieved
502 from
- 503 Feldhaar, H. (2011). Bacterial symbionts as mediators of ecologically important traits of
504 insect hosts. *Ecological Entomology*, 36(5), 533-543.
- 505 Fellous, S., & Salvaudon, L. (2009). How can your parasites become your allies? *Trends in*
506 *Parasitology*, 25(2), 62-66. doi:10.1016/j.pt.2008.11.010
- 507 Firth, L. B. (2017). Factors affecting the prevalence of the trematode parasite *Echinostephilla*
508 *patellae* (Lebour, 1911) in the limpet *Patella vulgata* (L.). *Journal of Experimental*
509 *Marine Biology and Ecology*, v. 492, pp. 99-104-2017 v.2492.
510 doi:10.1016/j.jembe.2017.01.026
- 511 Fischer, E. M., & Schär, C. (2010). Consistent geographical patterns of changes in high-
512 impact European heatwaves. *Nature Geoscience*, 3(6), 398-403.
513 doi:10.1038/ngeo866
- 514 Fitzhenry, T., Halpin, P. M., & Helmuth, B. (2004). Testing the effects of wave exposure, site,
515 and behavior on intertidal mussel body temperatures: applications and limits of
516 temperature logger design. *Marine Biology*, 145(2), 339-349. doi:10.1007/s00227-
517 004-1318-6
- 518 Futuyma, D. J., & Moreno, G. (1988). The evolution of ecological specialization. *Annual*
519 *Review of Ecology and Systematics*, 29, 207-233

- 520 Galis, F. (2001). Key innovations and radiations. *The character concept in evolutionary*
521 *biology*.
- 522 Garcia-Pichel, F., Ramírez-Reinat, E., & Gao, Q. (2010). Microbial excavation of solid
523 carbonates powered by P-type ATPase-mediated transcellular Ca²⁺ transport.
524 *Proceedings of the National Academy of Sciences*, 107(50), 21749-21754.
525 doi:10.1073/pnas.1011884108
- 526 Gehman, A.-L. M., Hall, R. J., & Byers, J. E. (2018). Host and parasite thermal ecology
527 jointly determine the effect of climate warming on epidemic dynamics. *Proceedings of*
528 *the National Academy of Sciences*, 115(4), 744-749.
- 529 Gehman, A.-L. M., & Harley, C. D. G. (2019). Symbiotic endolithic microbes alter host
530 morphology and reduce host vulnerability to high environmental temperatures.
531 *Ecosphere*, 10(4), e02683. doi:<https://doi.org/10.1002/ecs2.2683>
- 532 Gilman, S. E., Harley, C. D. G., Strickland, D. C., Vanderstraeten, O., O'Donnell, M. J., &
533 Helmuth, B. (2006). Evaluation of effective shore level as a method of characterizing
534 intertidal wave exposure regimes. *Limnol. Oceanogr. Methods*, 4, 448–445.
535 doi:<https://doi.org/10.4319/lom.2006.4.448>
- 536 Golubic, S., Radtke, G., & Le Campion-Alsumard, T. (2005). Endolithic fungi in marine
537 ecosystems. *Trends in Microbiology*, 13(5), 229-235.
- 538 Halpern, B. S., Walbridge, S., Selkoe, K. A., Kappel, C. V., Micheli, F., D'Agrosa, C., . . .
539 Watson, R. (2008). A global map of human impact on marine ecosystems. *Science*,
540 319(5865), 948-952. doi:10.1126/science.1149345
- 541 Harley, C. D. (2008). Tidal dynamics, topographic orientation, and temperature-mediated
542 mass mortalities on rocky shores. *Marine Ecology Progress Series*, 371, 37-46.
- 543 Harley, C. D. G. (2011). Climate change, keystone predation, and biodiversity loss. *Science*,
544 334(6059), 1124-1127. doi:10.1126/science.1210199
- 545 Harley, C. D. G., & Helmuth, B. S. T. (2003). Local- and regional-scale effects of wave
546 exposure, thermal stress, and absolute versus effective shore level on patterns of
547 intertidal zonation. *Limnol. Oceanogr.*, 48(4), 1498–1508.
548 doi:<https://doi.org/10.4319/lo.2003.48.4.1498>

- 549 Harvell, D., Altizer, S., Cattadori, I. M., Harrington, L., & Weil, E. (2009). Climate change and
550 wildlife diseases: When does the host matter the most? *Ecology*, 90(4), 912-920.
551 doi:10.1890/08-0616.1
- 552 Helmuth, B. (2002). How do we measure the environment? Linking intertidal thermal
553 physiology and ecology through biophysics. *Integrative and comparative biology*,
554 42(4), 837-845.
- 555 Helmuth, B., Broitman, B. R., Yamane, L., Gilman, S. E., Mach, K., Mislán, K. A. S., &
556 Denny, M. W. (2010). Organismal climatology: analyzing environmental variability at
557 scales relevant to physiological stress. *Journal of Experimental Biology*, 213(6), 995-
558 1003. doi:10.1242/jeb.038463
- 559 Helmuth, B., Choi, F., Matzelle, A., Torossian, J. L., Morello, S. L., Mislán, K. A. S., . . .
560 Zardi, G. (2016). Long-term, high frequency in situ measurements of intertidal mussel
561 bed temperatures using biomimetic sensors. *Scientific Data*, 3, 160087.
562 doi:10.1038/sdata.2016.87
- 563 Helmuth, B. S. T. (1998). Intertidal mussel microclimates: predicting the body temperature of
564 a sessile invertebrate. *Ecological Monographs*, 68(1), 51-74. doi:doi:10.1890/0012-
565 9615(1998)068[0051:IMMPTB]2.0.CO;2
- 566 Hobday, A. J., Oliver, E. C. J., Gupta, A. S., Benthuyssen, J. A., Burrows, M. T., Donat, M. G.,
567 . . . Smale, D. A. (2018). Categorizing and naming marine heatwaves.
568 *Oceanography*, 31(2), 162–173. doi:10.5670/oceanog.2018.205
- 569 Holbrook, N. J., Gupta, A. S., Oliver, E. C., Hobday, A. J., Benthuyssen, J. A., Scannell, H. A.,
570 . . . Wernberg, T. (2020). Keeping pace with marine heatwaves. *Nature Reviews*
571 *Earth & Environment*, 1-12.
- 572 Hughes, T. P., Kerry, J. T., Álvarez-Noriega, M., Álvarez-Romero, J. G., Anderson, K. D.,
573 Baird, A. H., . . . Berkelmans, R. (2017). Global warming and recurrent mass
574 bleaching of corals. *nature*, 543(7645), 373-377.
- 575 Hunter, J. P. (1998). Key innovations and the ecology of macroevolution. *Trends in ecology*
576 *& evolution*, 13(1), 31-36.

- 577 Janson, E. M., Stireman III, J. O., Singer, M. S., & Abbot, P. (2008). Phytophagous insect–
578 microbe mutualisms and adaptive evolutionary diversification. *Evolution: International*
579 *Journal of Organic Evolution*, 62(5), 997-1012.
- 580 Kaehler, S., & McQuaid, C. D. (1999). Lethal and sub-lethal effects of phototrophic endoliths
581 attacking the shell of the intertidal mussel *Perna perna*. *Marine Biology*, 135(3), 497-
582 503. doi:10.1007/s002270050650
- 583 Lafferty, K. D., & Holt, R. D. (2003). How should environmental stress affect the population
584 dynamics of disease? *Ecology Letters*, 6(7), 654-664.
- 585 Li, L., Hollowed, A. B., Cokellet, E. D., Barbeaux, S. J., Bond, N. A., Keller, A. A., . . .
586 Stabeno, P. J. (2019). Subregional differences in groundfish distributional responses
587 to anomalous ocean bottom temperatures in the northeast Pacific. *Global change*
588 *biology*, 25(8), 2560-2575.
- 589 Lourenço, C. R., Nicastro, K. R., McQuaid, C. D., Sabour, B., & Zardi, G. I. (2017).
590 Latitudinal incidence of phototrophic shell-degrading endoliths and their effects on
591 mussel bed microclimates. *Marine Biology*, 164(6), 129.
- 592 Macnab, V., & Barber, I. (2012). Some (worms) like it hot: fish parasites grow faster in
593 warmer water, and alter host thermal preferences. *Global change biology*, 18(5),
594 1540-1548.
- 595 Macreadie, P. I., Anton, A., Raven, J. A., Beaumont, N., Connolly, R. M., Friess, D. A., . . .
596 Duarte, C. M. (2019). The future of Blue Carbon science. *Nature communications*,
597 10(1), 3998. doi:10.1038/s41467-019-11693-w
- 598 Maga, E. A. (2020). UC Davis Transgenic Animal Research Conference XII (TARC XII).
599 *Transgenic Research*, 29(4), 461-465. doi:10.1007/s11248-020-00206-x
- 600 Marquet, N., Nicastro, K. R., Gektidis, M., McQuaid, C. D., Pearson, G. A., Serrão, E. A., &
601 Zardi, G. I. (2013). Comparison of phototrophic shell-degrading endoliths in invasive
602 and native populations of the intertidal mussel *Mytilus galloprovincialis*. *Biological*
603 *Invasions*, 15(6), 1253-1272. doi:10.1007/s10530-012-0363-1
- 604 Marshall, D. J., McQuaid, C. D., & Williams, G. A. (2010). Non-climatic thermal adaptation:
605 implications for species' responses to climate warming. *Biology Letters*, 6(5), 669-
606 673. doi:10.1098/rsbl.2010.0233

- 607 Met Office. (2019a). MIDAS Open: UK hourly rainfall data, v201908. *Centre for*
608 *Environmental Data Analysis*, 30 October 2019.
609 doi:<https://doi.org/10.5285/a58b9c8a724e4ec795a40a74455462b7>
- 610 Met Office. (2019b). MIDAS Open: UK hourly solar radiation data, v201908. *Centre for*
611 *Environmental Data Analysis*, 30 October 2019.
612 doi:<https://doi.org/10.5285/d6bbe115245042dc93ee68caa253d60b>
- 613 Met Office. (2019c). MIDAS Open: UK hourly weather observation data, v201908. *Centre for*
614 *Environmental Data Analysis*, 30 October 2019.
615 doi:<https://doi.org/10.5285/6c441aea187b44819b9e929e575b0d7e>
- 616 Miller, A. H. (1949). Some ecologic and morphologic considerations in the evolution of higher
617 taxonomic categories. *Ornithologie als biologische Wissenschaft*, 28, 84-88.
- 618 Miller, L. P., & Dowd, W. W. (2017). Multimodal in situ datalogging quantifies inter-individual
619 variation in thermal experience and persistent origin effects on gaping behavior
620 among intertidal mussels (*Mytilus californianus*). *Journal of Experimental Biology*,
621 220(22), 4305-4319.
- 622 Moyon, N. E., Somero, G. N., & Denny, M. W. (2019). Impact of heating rate on cardiac
623 thermal tolerance in the California mussel, *Mytilus californianus*. *Journal of*
624 *Experimental Biology*, 222(17), jeb203166.
- 625 Ndhlovu, A., McQuaid, C. D., & Monaco, C. J. (2021). Ectoparasites reduce scope for growth
626 in a rocky-shore mussel (*Perna perna*) by raising maintenance costs. *Science of The*
627 *Total Environment*, 753, 142020. doi:<https://doi.org/10.1016/j.scitotenv.2020.142020>
- 628 Ndhlovu, A., McQuaid, C. D., Nicastro, K., Marquet, N., Gektidis, M., Monaco, C. J., & Zardi,
629 G. (2019). Biogeographical Patterns of Endolithic Infestation in an Invasive and an
630 Indigenous Intertidal Marine Ecosystem Engineer. *Diversity*, 11(5), 75.
- 631 Ndhlovu, A., McQuaid, C. D., Nicastro, K. R., & Zardi, G. I. (2020). Community succession in
632 phototrophic shell-degrading endoliths attacking intertidal mussels. *Journal of*
633 *Molluscan Studies*. doi:10.1093/mollus/eyaa036
- 634 Nicastro, K. R., McQuaid, C. D., Diebart, A., & Zardi, G. I. (2020). Intraspecific diversity in an
635 ecological engineer functionally trumps interspecific diversity in shaping community

- 636 structure. *Science of The Total Environment*, 743, 140723.
637 doi:<https://doi.org/10.1016/j.scitotenv.2020.140723>
- 638 Nicastro, K. R., McQuaid, C. D., & Zardi, G. I. (2018). Between a rock and a hard place:
639 combined effect of trampling and phototrophic shell-degrading endoliths in marine
640 intertidal mussels. *Marine Biodiversity*, 1-6.
- 641 Nicastro, K. R., Zardi, G. I., McQuaid, C. D., Pearson, G. A., & Serrão, E. A. (2012). Love
642 Thy Neighbour: Group Properties of Gaping Behaviour in Mussel Aggregations.
643 *PLoS One*, 7(10), e47382. doi:<https://doi.org/10.1371/journal.pone.0047382>
- 644 Nowakowski, A. J., Whitfield, S. M., Eskew, E. A., Thompson, M. E., Rose, J. P., Caraballo,
645 B. L., . . . Todd, B. D. (2016). Infection risk decreases with increasing mismatch in
646 host and pathogen environmental tolerances. *Ecology Letters*, 19(9), 1051-1061.
- 647 Oliver, E. C., Donat, M. G., Burrows, M. T., Moore, P. J., Smale, D. A., Alexander, L. V., . . .
648 Hobday, A. J. (2018). Longer and more frequent marine heatwaves over the past
649 century. *Nature communications*, 9(1), 1-12.
- 650 Perkins-Kirkpatrick, S. E., & Lewis, S. C. (2020). Increasing trends in regional heatwaves.
651 *Nature communications*, 11(1), 3357. doi:10.1038/s41467-020-16970-7
- 652 Petes, L. E., Menge, B. A., & Murphy, G. D. (2007). Environmental stress decreases
653 survival, growth, and reproduction in New Zealand mussels. *Journal of Experimental*
654 *Marine Biology and Ecology*, 351(1-2), 83-91.
- 655 Pinheiro, J., Bates, D., DebRoy, S., Sarkar, D., & R Core Team. (2020). nlme: Linear and
656 Nonlinear Mixed Effects Models. <https://CRAN.R-project.org/package=nlme>: R
657 package version 3.1-151.
- 658 Pittera, J., Humily, F., Thorel, M., Grulois, D., Garczarek, L., & Six, C. (2014). Connecting
659 thermal physiology and latitudinal niche partitioning in marine *Synechococcus*. *The*
660 *ISME journal*, 8(6), 1221-1236.
- 661 Porter, W. P., & Gates, D. M. (1969). Thermodynamic Equilibria of Animals with
662 Environment. *Ecol. Monogr.*, 39(3), 227-244. doi:<https://doi.org/10.2307/1948545>
- 663 Rabosky, D. L. (2014). Automatic detection of key innovations, rate shifts, and diversity-
664 dependence on phylogenetic trees. *PLoS One*, 9(2), e89543.

- 665 Raffaelli, D., & Hawkins, S. J. (2012). *Intertidal ecology*. Springer Science & Business Media.
- 666 Rahmstorf, S., & Coumou, D. (2011). Increase of extreme events in a warming world.
667 *Proceedings of the National Academy of Sciences*, 108(44), 17905.
668 doi:10.1073/pnas.1101766108
- 669 Reyes-Nivia, C., Diaz-Pulido, G., Kline, D., Guldberg, O. H., & Dove, S. (2013). Ocean
670 acidification and warming scenarios increase microbioerosion of coral skeletons.
671 *Global change biology*, 19(6), 1919-1929.
- 672 Santos, J. C., Coloma, L. A., & Cannatella, D. C. (2003). Multiple, recurring origins of
673 aposematism and diet specialization in poison frogs. *Proceedings of the National*
674 *Academy of Sciences*, 100(22), 12792-12797.
- 675 Sauer, E. L., Fuller, R. C., Richards-Zawacki, C. L., Sonn, J., Sperry, J. H., & Rohr, J. R.
676 (2018). Variation in individual temperature preferences, not behavioural fever, affects
677 susceptibility to chytridiomycosis in amphibians. *Proceedings of the Royal Society B:*
678 *Biological Sciences*, 285(1885), 20181111.
- 679 Schuster, S., Wöhl, S., Griebisch, M., & Klostermeier, I. (2006). Animal cognition: how archer
680 fish learn to down rapidly moving targets. *Current Biology*, 16(4), 378-383.
- 681 Seabra, R., Wetthey, D. S., Santos, A. M., & Lima, F. P. (2015). Understanding complex
682 biogeographic responses to climate change. *Scientific Reports*, 5(1), 1-6.
- 683 Seuront, L., Nicastro, K. R., Zardi, G. I., & Goberville, E. (2019). Decreased thermal
684 tolerance under recurrent heat stress conditions explains summer mass mortality of
685 the blue mussel *Mytilus edulis*. *Scientific Reports*, 9(1), 17498. doi:10.1038/s41598-
686 019-53580-w
- 687 Smale, D. A., Wernberg, T., Oliver, E. C. J., Thomsen, M., Harvey, B. P., Straub, S. C., . . .
688 Moore, P. J. (2019). Marine heatwaves threaten global biodiversity and the provision
689 of ecosystem services. *Nature Climate Change*, 9(4), 306-312. doi:10.1038/s41558-
690 019-0412-1
- 691 Stillman, J. H. (2019). Heat Waves, the New Normal: Summertime Temperature Extremes
692 Will Impact Animals, Ecosystems, and Human Communities. *Physiology*, 34(2), 86-
693 100. doi:10.1152/physiol.00040.2018

- 694 Suchanek, T. (1985). Mussels and their role in structuring rocky shore communities. *The*
695 *Ecology of Rocky Coastes*, 70-96.
- 696 Summers, K. (2003). Convergent evolution of bright coloration and toxicity in frogs.
697 *Proceedings of the National Academy of Sciences*, 100(22), 12533-12534.
- 698 Tribollet, A., Godinot, C., Atkinson, M., & Langdon, C. (2009). Effects of elevated pCO₂ on
699 dissolution of coral carbonates by microbial euendoliths. *Global Biogeochemical*
700 *Cycles*, 23(3).
- 701 Tsuchiya, M. (1983). Mass mortality in a population of the mussel *Mytilus edulis* L. caused
702 by high temperature on rocky shores. *Journal of Experimental Marine Biology*
703 *Ecology*, 66, 101-111.
- 704 Wernberg, T., Smale, D. A., Tuya, F., Thomsen, M. S., Langlois, T. J., de Bettignies, T., . . .
705 Rousseaux, C. S. (2013). An extreme climatic event alters marine ecosystem
706 structure in a global biodiversity hotspot. *Nature Clim. Change*, 3(1), 78-82.
707 doi:[http://www.nature.com/nclimate/journal/v3/n1/abs/nclimate1627.html#supplement](http://www.nature.com/nclimate/journal/v3/n1/abs/nclimate1627.html#supplementary-information)
708 [ary-information](http://www.nature.com/nclimate/journal/v3/n1/abs/nclimate1627.html#supplementary-information)
- 709 Zardi, G., Nicastro, K., McQuaid, C., Ng, T., Lathlean, J., & Seuront, L. (2016). Enemies with
710 benefits: parasitic endoliths protect mussels against heat stress. *Scientific Reports*, 6,
711 31413.
- 712 Zardi, G. I., Nicastro, K. R., McQuaid, C. D., & Gektidis, M. (2009). Effects of endolithic
713 parasitism on invasive and indigenous mussels in a variable physical environment.
714 *PLoS One*, 4(8), e6560.
- 715
- 716

717 **TABLES**

718 **Table 1. Main drivers of the maximum difference in body temperature between non-**
 719 **infested and infested mussels.** Results are shown for all best candidate models ($\Delta AICc <$
 720 2) as compared to the null model, along with associated Akaike weights (relative support of
 721 each model). The selected model (least number of parameters) is indicated in bold.

Meteorological parameters (estimated coefficients \pm SE)	AICc	$\Delta AICc$	Akaike weights
Intercept(0.51 \pm 0.35) + AT(-0.03 \pm 0.02) + SR(0.05 \pm 0.005) + WS(-0.04 \pm 0.01) + Rdm(SD=0.24)	1845.13	0	0.28
Intercept(0.09\pm0.16) + SR(0.05\pm0.005) + WS(-0.04\pm0.01) + Rdm(SD=0.24)	1845.34	0.21	0.25
Intercept(0.66 \pm 0.36) + SR(0.04 \pm 0.007) + RH(-0.006 \pm 0.004) + WS(-0.04 \pm 0.01) + Rdm(SD=0.24)	1845.88	0.75	0.19
Intercept(0.94 \pm 0.48) + AT(-0.02 \pm 0.02) + SR(0.05 \pm 0.007) + RH(-0.005 \pm 0.004) + WS(-0.04 \pm 0.01) + Rdm(SD=0.25)	1846.14	1.02	0.17
Intercept(0.50 \pm 0.35) + AT(-0.03 \pm 0.02) + SR(0.05 \pm 0.005) + PR(0.002 \pm 0.005) + WS(-0.04 \pm 0.01) + Rdm(SD=0.24)	1847.01	1.88	0.11
null	1969.24	124.12	0

722 Abbreviations: Solar Radiation (SR), Relative Humidity (RH), Wind Speed (WS), Air
 723 Temperature (AT) and Precipitation (PR), Random factor (Rdm; robomussel identity nested
 724 within locations).

725

726 **Table 2. Meteorological conditions during heatwaves identified in 2018 at Wimereux,**
 727 **France.** Heat waves were identified based on air temperature during summer 2018, and were
 728 classified from moderate to extreme: “These events were classified as moderate (78.1%) to
 729 strong (21.9%) in June, moderate (67.8%), strong (23.1%), severe (7.0%) and extreme (2.0%)
 730 in July, and moderate (63.0%), strong (30.9%) and severe (6.2%) in August.” (from Seuront
 731 et al. 2019). Maximum temperature differences between non-infested and infested mussels

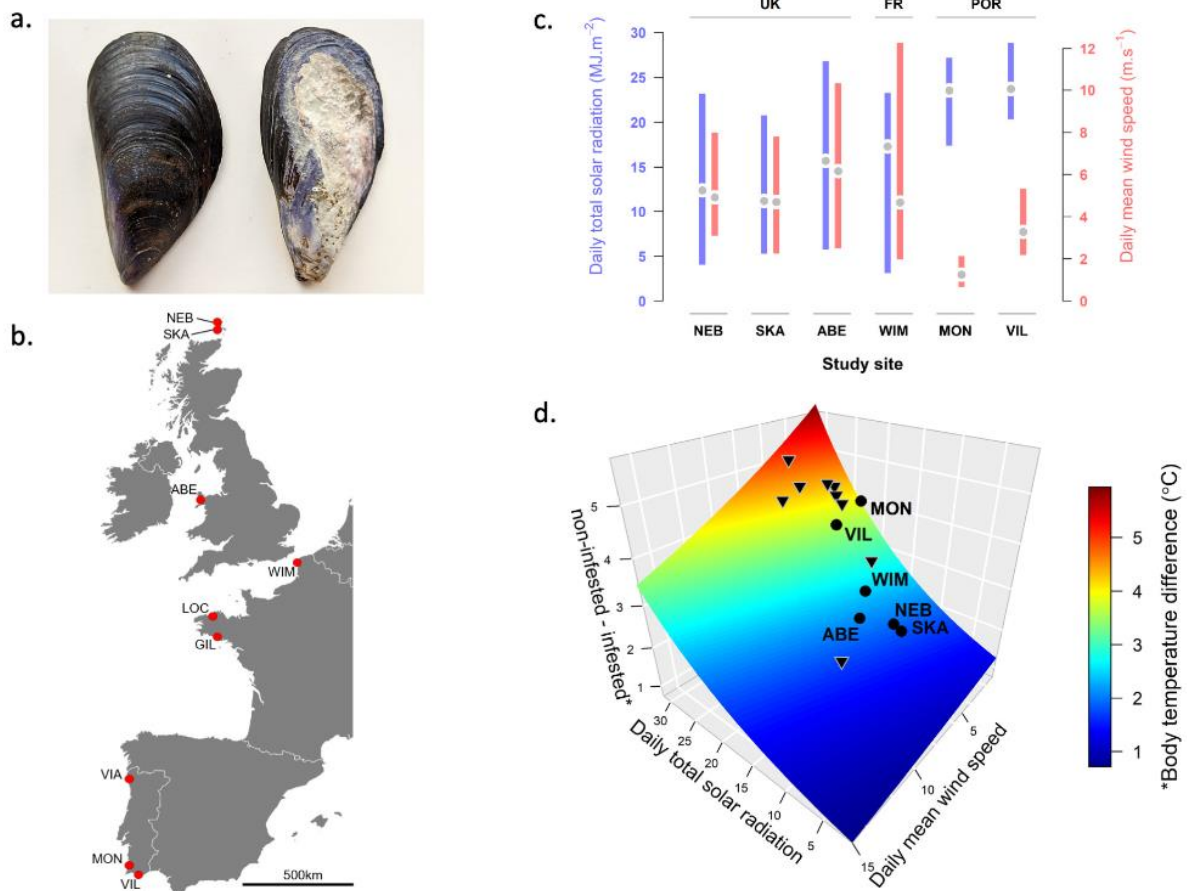
732 were predicted based on wind speed and solar radiation using the model selected in the
 733 present study.

Date (in 2018)	Mean daily wind speed (m.s ⁻¹)	Mean daily total solar radiation (MJ.m ⁻²)	Predicted max. temperature differences (°C) (95% confidence intervals)
June 28 to 30	4.54	28.160	4.26 (1.15)
July 05 to 07	2.48	26.006	4.14 (1.12)
July 23 to 25	2.61	24.433	3.80 (1.11)
August 01 to 08	2.67	25.350	3.97 (1.11)
June 23	2.81	26.610	4.21 (1.13)
June 26	4.41	30.270	4.77 (1.17)
July 13	3.12	18.510	2.75 (1.08)
July 17	5.95	28.350	4.06 (1.17)
August 10	8.95	13.340	1.67 (1.12)

734

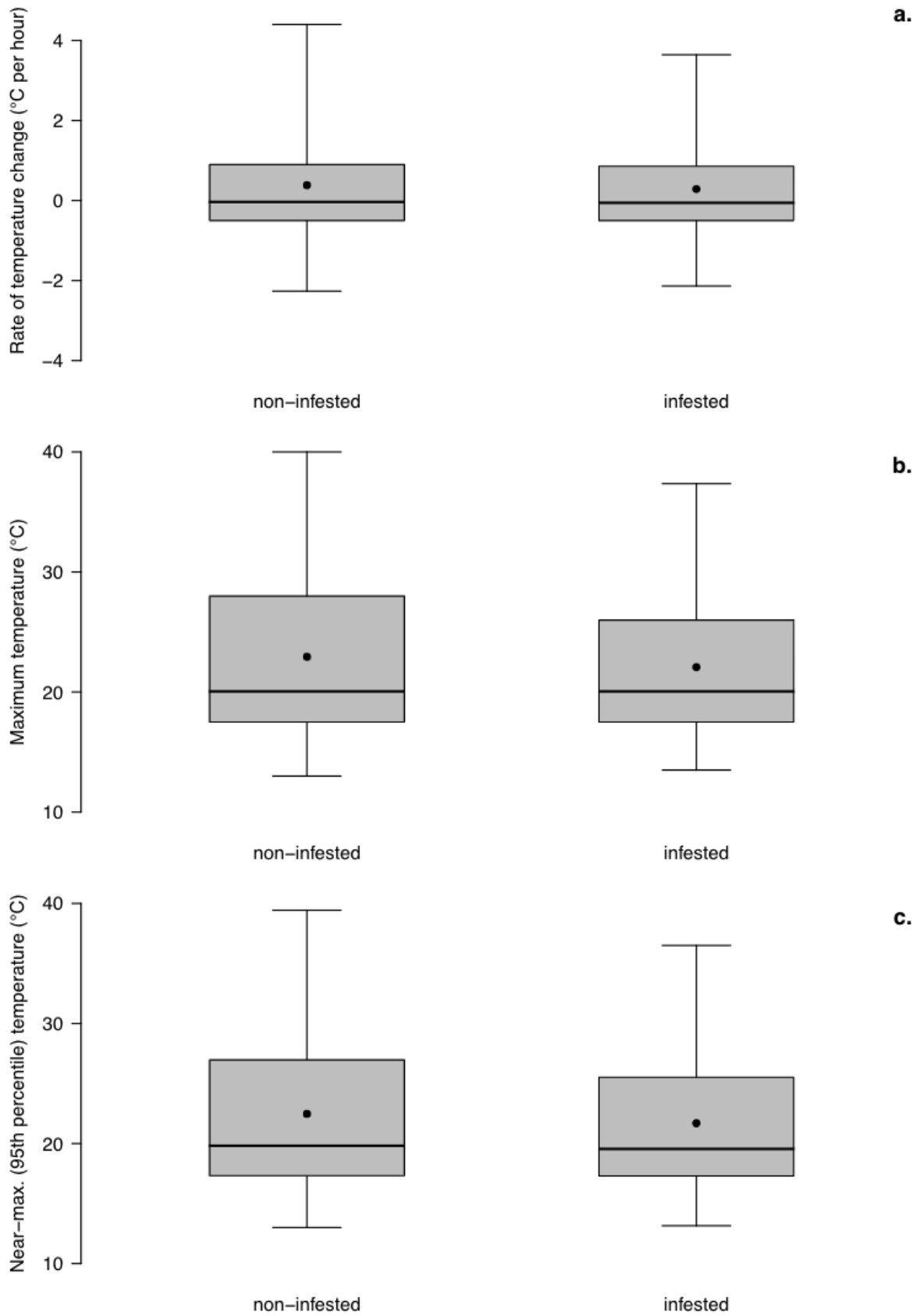
735

736 **FIGURE LEGENDS**



737

738 **Fig. 1.** (a) Example of non-infested and infested mussels. (b) Study sites where mussels were
739 deployed. (c) Daily total (global) solar radiation (blue) and mean wind speed (red) during
740 emergence at (from north (left) to south (right)) Nebo Geo (NEB), Bay of Skail (SKA) and
741 Aberffraw (ABE), United Kingdom (UK), Wimereux (WIM), France (FR) and, Monte Clerigo
742 (MON) and Vilamoura (VIL), Portugal (POR). Coloured bars indicate 2.5th and 97.5th
743 percentiles and grey points are the median values. (d) Prediction surface of maximum
744 temperature differences in body temperature between non-infested and infested mussels (see
745 Supplementary Fig. S2 for a 2D representation with confidence intervals): The daily maximum
746 difference increases with increasing solar radiation and decreasing wind speed (units are
747 displayed in panel c). Black points indicate the mean expected difference for each site using
748 data averaged over the study period and triangles indicate the mean expected difference
749 during nine heatwaves identified at Wimereux during summer 2018 (confidence intervals are
750 between +/-1.08°C and +/-1.15°C for predictions during heatwaves; see Table 2).



752 **Fig. 2. Comparison of the temperature response between non-infested and infested**
753 **mussels.** (a) Average rate of change in body temperatures and (b) maximum or (c) near-
754 maximum (95th percentile) temperatures (per tidal cycles) during emergence. Means (black
755 dots), medians (central bars), 2.5th and 97.5th percentiles (respectively, lower and upper bars),
756 and 25th and 75th percentiles (grey boxes) are shown.

757

758